Optimal Data Analysis
2010, Vol. 1, Release 1 (September 17, 2010), 67-100

2155-0182/10/$3.00

The Use of Unconfounded Climatic Data Improves Atmospheric Prediction

Robert C. Soltysik, M.S., and Paul R. Yarnold, Ph.D.
Optimal Data Analysis, LLC

This report improves measurement properties of data and analytic methods widely used in meteorological modeling and forecasting. Paradoxical confounding is defined and demonstrated using global temperature land-ocean index data. It is shown that failure to address paradoxical confounding results in suboptimal atmospheric circulation pattern models, and correcting prior measurement and analytic deficiencies results in more accurate prediction of temperature and precipitation anomalies, and export of Arctic sea ice.

Simpson's Paradox may be the single greatest threat to the validity of quantitative analysis in all empirical science.[1] The Paradox can occur when data from two or more samples, groups or time periods are combined into a single sample: under such conditions, results obtained when analyzing the combined data may be different than when analyzing individual data sets separately. The following hypothetical example illustrates confounding for a simple correlation.

Imagine we wish to correlate sea level pressure (SLP) with thunderstorm severity rated using a scale with greater values indicating greater severity, and data collected at two locations. Location A usually has relatively low SLP and short-lived, fast-moving storms: the lower the SLP the more severe the storm. The hypothetical correlation model (r=-0.8) relating SLP and severity is indicated using arrow "**A**" in Figure 1 (individual hypothetical data points from location A are indicated as "a"): data swarm A indicates strong *negative* association.

Compared to A, Location B usually has relatively high SLP and long-lived slow-moving storms: the lower the SLP the more severe the storm. The correlation (r=-0.8) relating SLP and severity is indicated in Figure 1 by arrow "**B**" (individual hypothetical data points from location B are indicated as "b"): data swarm B indicates strong *negative* association.

When data from Locations A and B are combined, the resulting correlation model (r= 0.7) relating SLP and severity is indicated by arrow "**C**" (individual hypothetical data points for combined sample are all "a" and "b"): data swarm C indicates strong *positive* association.

In this hypothetical example, for two individual samples (Locations A and B) considered separately the analysis reveals that more severe storms are associated with *decreasing* SLP. For the combined data, the same analysis reveals that more severe storms are associated with *increasing* SLP.

2155-0182/10/$3.00

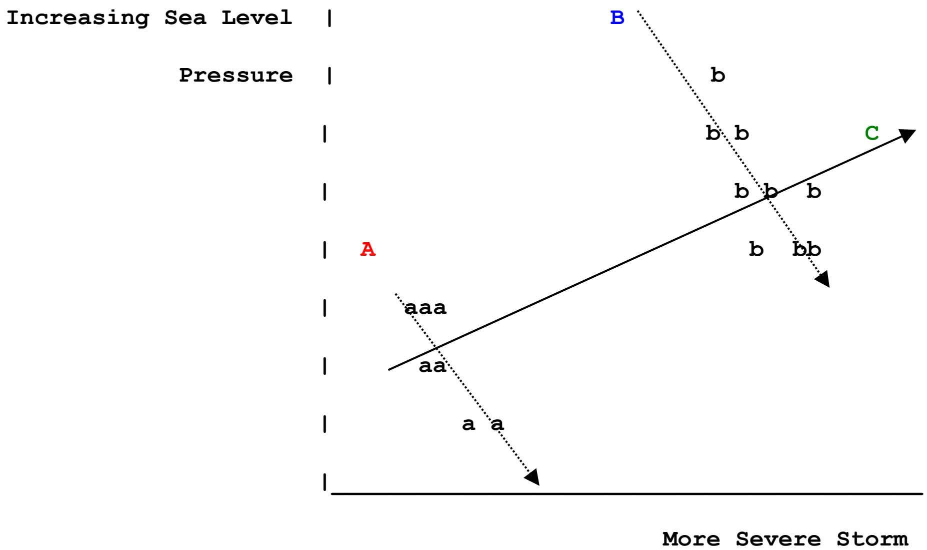

Figure 1: Hypothetical Illustration of Paradoxical Confounding

Simpson's Paradox threatens the validity of quantitative atmospheric science because nonstationarity is prevalent in longitudinal data series used in atmospheric science, such as temperature or pressure—and nonstationarity can induce Simpson's Paradox. For example, global surface temperature data clearly are nonstationary: in Figure 2, anomalies are computed relative to the period 1951-1980 (http://data.giss.nasa.gov/gistemp/).

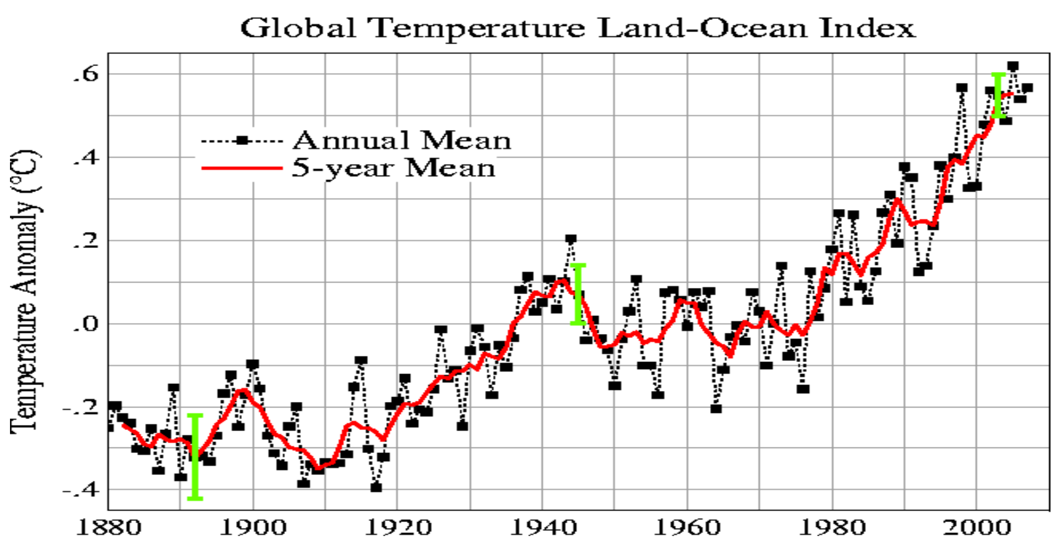

Figure 2: Mean Global Temperature Land-Ocean Index Anomaly by Year

2155-0182/10/$3.00

Analysis was restricted to the time period that is the focus of most current quantitative atmospheric science, beginning in the year 1948. Eyeball inspection of Figure 2 suggests a relatively flat trajectory ("*stationary series*") through 1976, versus a steadily increasing trajectory ("*non-stationary series*") across subsequent years. Regression analyses modeling temperature anomaly (dependent measure) as a function of year (independent measure), separately by month, are summarized In Table 1: findings confirm eyeball observations, and establish the generalizability of the phenomenon to a time period more granular than is afforded by annual measurements.

Tabled for each model is the intercept as well as the value of the t-test for the two-tailed hypothesis that the value of the intercept is zero, and the associated Type I error rate. For every model, in every month, the intercept is *not* significantly different than zero for the stationary series, but *is* significantly different than zero for the nonstationary and combined series. Also tabled for each model is the slope (regression beta weight) and the value of the t-test for the two-tailed hypothesis that the value of the slope is zero, and the associated Type I error rate. Consistent with findings for intercept, for every model, in every month, the slope is *not* significantly different than zero for the stationary series, but *is* significantly different than zero for the nonstationary and combined series. Finally, Table 1 provides the percent of variance in temperature that is explained by the regression model as a function of year (R^2), and p for the regression model. If model performance for the combined sample lies outside performance results for samples considered individually, then paradoxical confounding exists: this is indicated using **red**.

Table 1: Regression Modeling of Temperature Anomaly using Year, Separately by Month: Evidence of Paradoxical Confounding

Month	Time Period	Intercept	t	*p*	Slope	t	*p*	R^2	*p*
January	Stationary	559.3	0.8	0.45	-0.29	-0.8	0.46	2.1	0.45
	Non-Stationary	-3239.1	-5.3	0.0001	1.64	5.3	0.0001	49.4	0.0001
	Combined	-2114.5	-7.9	0.0001	1.08	8.0	0.0001	52.2	0.0001
February	Stationary	-140.0	-0.2	0.87	0.07	0.2	0.87	1.0	0.87
	Non-Stationary	-3842.6	-5.5	0.0001	1.95	5.6	0.0001	51.6	0.0001
	Combined	-2451.3	-8.4	0.0001	1.25	8.5	0.0001	55.3	0.0001
March	Stationary	-550.5	-0.8	0.46	0.28	0.8	0.46	2.1	0.46
	Non-Stationary	-3374.5	-5.9	0.0001	1.71	5.9	0.0001	54.9	0.0001
	Combined	-2451.8	-10.0	0.0001	1.25	10.1	0.0001	63.8	0.0001
April	Stationary	-229.4	-0.4	0.71	0.12	0.4	0.72	0.5	0.72
	Non-Stationary	-3216.2	-7.1	0.0001	1.63	7.1	0.0001	63.7	0.0001
	Combined	-2159.7	-10.3	0.0001	1.10	10.4	0.0001	65.0	0.0001
May	Stationary	-197.5	-0.3	0.75	0.10	0.3	0.75	0.4	0.75
	Non-Stationary	-2590.9	-4.9	0.0001	1.31	4.9	0.0001	45.4	0.0001
	Combined	-1845.2	-8.6	0.0001	0.94	8.7	0.0001	56.7	0.0001
June	Stationary	-145.7	-0.3	0.75	0.07	0.3	0.75	0.4	0.75
	Non-Stationary	-3291.0	-6.3	0.0001	1.67	6.4	0.0001	58.3	0.0001
	Combined	-1918.6	-9.7	0.0001	0.98	9.7	0.0001	62.0	0.0001

2155-0182/10/$3.00

July	**Stationary**	-111.3	-0.3	0.78	0.06	0.3	0.79	0.3	0.79
	Non-Stationary	-2841.5	-4.7	0.0001	1.44	4.8	0.0001	43.8	0.0001
	Combined	-1937.1	-9.5	0.0001	0.99	9.6	0.0001	61.3	0.0001
August	**Stationary**	203.2	0.4	0.73	-0.10	-0.4	0.73	0.5	0.73
	Non-Stationary	-3492.9	-6.5	0.0001	1.77	6.6	0.0001	60.0	0.0001
	Combined	-1933.3	-8.5	0.0001	0.98	8.6	0.0001	55.8	0.0001
September	**Stationary**	3.9	0.0	0.99	-0.01	-0.0	0.99	0.1	0.99
	Non-Stationary	-3359.2	-6.3	0.0001	1.70	6.4	0.0001	58.4	0.0001
	Combined	-1888.2	-8.8	0.0001	0.96	8.8	0.0001	57.3	0.0001
October	**Stationary**	298.4	0.6	0.58	-0.15	-0.6	0.58	1.2	0.58
	Non-Stationary	-4082.0	-8.5	0.0001	2.06	8.5	0.0001	71.4	0.0001
	Combined	-1920.6	-8.5	0.0001	0.98	8.5	0.0001	55.7	0.0001
November	**Stationary**	-253.9	-0.5	.062	0.13	0.5	0.62	0.9	0.62
	Non-Stationary	-3719.7	-6.1	0.0001	1.88	6.1	0.0001	56.3	0.0001
	Combined	-2056.9	-9.1	0.0001	1.05	9.1	0.0001	58.9	0.0001
December	**Stationary**	41.4	0.1	0.95	-0.02	-0.7	0.95	0.1	0.95
	Non-Stationary	-3076.1	-5.0	0.0001	1.56	5.1	0.0001	45.1	0.0001
	Combined	-1998.4	-8.2	0.0001	1.02	8.3	0.0001	54.2	0.0001

Note: Stationary=1948–1976; Non-Stationary=1977–2007; Combined=1948-2007.

This exercise demonstrates that temperature does *not* increase between 1948 and 1976, but *does* increase thereafter; fundamentally different "statistical infrastructure" (i.e., regression models) underlies the stationary and nonstationary series; and combining data from these two series typically results in paradoxical confounding. What is the nature of the effect of this confounding? In the initial hypothetical example, the effect of the confounding was one of "direction": the result for the combined sample was opposite in direction to results obtained for individual samples. For actual temperature data the effect of confounding is one of "magnitude": the finding for the combined sample is in the same direction (indicating increase over time) as the finding for the nonstationary series, but the model for the combined sample misestimates the magnitude of the effect. For any month, compared to the nonstationary series, the model for the combined sample has intercept and slope coefficients with lower absolute values: models for the combined data thus underestimate the rate of change in temperature for the nonstationary series. *If Simpson's Paradox confounds fundamental data, then models using those confounded data also are confounded*.

Measuring Atmospheric Circulation Patterns

Seminal research conducted by Barnston and Livezey used orthogonally rotated principal components analysis (PCA) of monthly mean 700 mb geopotential heights to identify the major modes of northern hemisphere upper-air variability.[2] They used combined data from the years 1950 through 1984: measurements were taken on a 358-point grid covering latitudes from 20ºN to 85ºN, and ten "robust" modes (components) were identified which persisted throughout the year. The Climate Prediction Center (CPC) performed a similar analysis of northern hemisphere 500 mb heights using data from 1950 to 2000: ten modes were identified and used to compute the values of the teleconnection indices (http://www.cpc.noaa.gov/data/teledoc/telepatcalc.shtml). Table 2 describes the ten modes of upper-air variability determined by the CPC analysis.

2155-0182/10/$3.00

Table 2: Ten Modes of Upper-Air Variability Determined by the CPC Analysis

CPC Mode	Abbreviation	Description
1	NAO	North Atlantic Oscillation
2	EA	East Atlantic Pattern
3	WP	West Pacific Pattern
4	EP/NP	East Pacific / North Pacific Pattern
5	PNA	Pacific / North American Pattern
6	EA/WR	East Atlantic/West Russia Pattern
7	SCA	Scandinavia Pattern
8	TNH	Tropical / Northern Hemisphere Pattern
9	POL	Polar/ Eurasia Pattern
10	PT	Pacific Transition Pattern

Figure 3 gives the total variance in 500 mb height data that is explained by these ten modes each year. In the Figure, blue shading indicates levels of explained variation that fall below the mean. In 2003 the combined sample includes an equal number of data points from stationary (1950-1976) and nonstationary (1977-2003) series, but data from the nonstationary series dominate the combined sample by 2004. Extrapolation of earlier results suggests that increasing domination will accelerate paradoxical confounding and resulting underestimation of magnitude of effect. Note that after 2003, *performance of the quantitative model used to identify major modes of northern hemisphere upper-air variability has never been lower*.

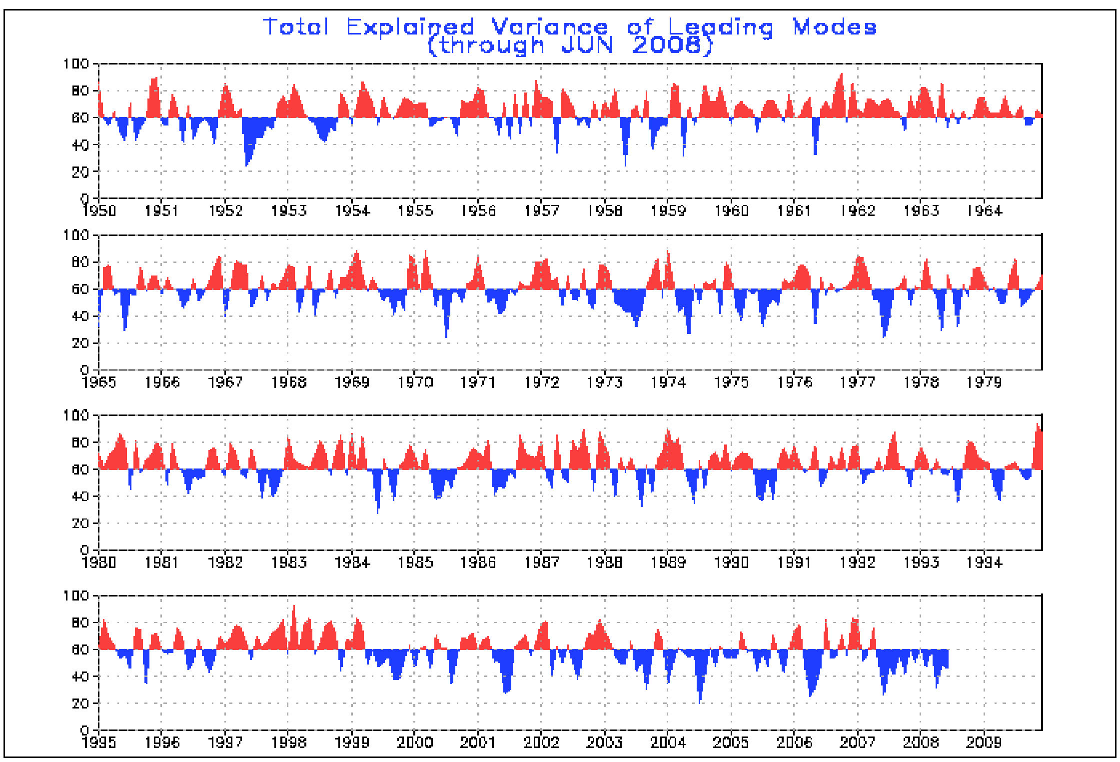

Figure 3: Variance in 500mb Height Data Explained by 10 CPC Modes, by Year

2155-0182/10/$3.00

It is simple to show that this accelerating failure of the current state-of-the-art is in part attributable to paradoxical confounding. We obtained January 500 mb geopotential height data from 1948-2007 from the NCEP/NCAR Reanalysis dataset, for the full 379-point grid used in research cited earlier, separating the data into stationary (1948-1976) versus nonstationary (1977-2007) series (http://www.cdc.noaa.gov/cgi-bin/Timeseries/timeseries1.pl). We replicated prior varimax-rotated, ten-extracted-factor PCA of 500 mb height data (see Table 3). The principal component column indicates successive eigenvector (mode). For Sample, S is the stationary series, NS the non-stationary series, and C the combined S and NS data. Eigenvalue is given for each sample and mode, as is corresponding percent of total variance explained by the mode. For example, the first mode for the stationary series had an eigenvalue of 68.1, thus explaining 18.0% of the total variance of 379 measurements of 500 mb heights. Indicated using **red**, paradoxical confounding exists when the eigenvalue for the C sample falls outside of the domain defined by the S and NS samples. Note that 80% of the modes clearly reveal paradoxical confounding: in every case except mode number 2 the effect was underestimation of explained variation.

Table 3: Replication of Prior Analysis of January 500 mb Geopotential Height Data, Separately by Series

Principal Component	Sample	Eigenvalue	Percent of Variance	Cumulative Percent Variance
1	S	68.1	18.0	18.0
	NS	75.3	19.9	19.9
	C	63.3	16.7	16.7
2	S	58.0	15.3	33.3
	NS	50.2	13.3	33.1
	C	60.0	15.8	32.5
3	S	42.0	11.1	44.4
	NS	39.1	10.3	43.4
	C	32.4	8.6	41.1
4	S	37.4	9.9	54.2
	NS	34.2	9.0	52.5
	C	29.5	7.8	48.9
5	S	24.8	6.5	60.8
	NS	27.3	7.2	59.7
	C	27.0	7.1	56.0
6	S	23.9	6.3	67.1
	NS	22.7	6.0	65.7
	C	21.0	5.5	61.5
7	S	18.6	4.9	72.0
	NS	19.6	5.2	70.8
	C	18.1	4.8	66.3

8	S	16.1	4.2	76.2
	NS	15.4	4.1	74.9
	C	13.4	3.5	69.8
9	S	13.7	3.6	79.8
	NS	15.3	4.0	78.9
	C	12.5	3.3	73.1
10	S	13.2	3.5	83.3
	NS	11.0	2.9	81.8
	C	11.4	3.0	76.2

Table 3 also provides the *cumulative* percent of total variance (of 379 variables) explained by the modes for each sample, across successive modes. Indicated using **blue**, paradoxical confounding exists when the cumulative value of this performance index for the C sample falls outside of the domain defined by the S and NS samples. *All* factors clearly reveal paradoxical confounding, and the effect was always underestimation of explained variation.

In addition to examining omnibus performance results of the current ten-mode solution, it is instructive to examine internal measurement properties of the individual modes. If the structure underlying the modes (reflected by the relationship of the 379 measurements of 500 mb heights to the mode score) is parallel, then the mode scores for the S, NS and C samples will be internally consistent (i.e., measure the same underlying construct), and a one-factor PCA of the three mode scores should explain most of the variation (theoretical maximum=100%), coefficient Alpha (positively related to the mean item-total correlation and the number of measures in the index) for the resulting factor score should be high (theoretical maximum=1.0), and the root-mean-squared-residual, or RMSR (an index of the average error in estimating the actual inter-measure correlation based on the mode structure) of the resulting factor score should be low (theoretical minimum=0). Seen below, the ten confounded current modes have poor internal measurement properties even by social science standards—for example, for personality surveys with modes measured using a fraction as many measures.[3]

Table 4: Internal Measurement Properties of Ten CPC Modes

Principal Component	Eigenvalue	Percent of Variance	Alpha	RMSR
1	1.89	63.3	0.710	0.2772
2	1.82	60.5	0.674	0.2913
3	2.22	74.1	0.825	0.1749
4	1.71	57.1	0.625	0.2744
5	1.54	51.4	0.527	0.2771
6	1.42	47.2	0.440	0.1812

2155-0182/10/$3.00

7	1.45	48.5	0.469	0.3011
8	1.96	65.2	0.734	0.1805
9	1.63	54.2	0.577	0.2293
10	1.56	52.0	0.539	0.2404

Empirical results clearly demonstrate that current state-of-the-art models of modes of northern hemisphere upper-air variability are confounded by Simpson's paradox, underestimate model performance and phenomenon effect strength, and produce modes having poor measurement properties. Because data for only one month were used in this demonstration, these analyses represent a "best case scenario." Prior research first smoothed data over successive three month periods prior to conducting PCA: because the reliability of a composite exceeds the reliability of the constituents, smoothed scores will result in lower volatility (i.e., less extreme outliers) and weaker inter-measure correlations, eigenvalues, and measurement properties.

Theoretical consideration of current state-of-the-art models of modes also is not compelling. First, current modes are *non-granular*: postulating that a total of only ten modes underlie northern hemisphere upper-air variability is relatively simplistic compared with complexity underlying many large natural systems. Second, current modes are *nonparsimonious*, because computing an omnibus mode score requires (in the scoring formula) the use of all geopotential height measures. Third, low parsimony makes current mode scores robust: because many constituents (grid locations) are included in the scoring formula, positive changes in some constituents are offset by negative changes in others, so mode scores are *insensitive*. Finally, by formulation PCA is designed to produce *linear* models (modes), yet the present results failed to reveal strong linear modes as indicated by modest eigenvalues: there is therefore discordance between methodology (PCA), data (paradoxically confounded), method (how PCA was conducted), and objective (identifying psychometrically sound measures of major modes of northern hemisphere upper-air variability).

Unconfounded Measurement of Major Modes

Theoretical and empirical limitations of the original solution motivated development of a new methodology for identifying superior modes, which eliminates problems discussed earlier. Our proprietary method constitutes a theoretical shift in the way teleconnections are conceptualized, and a search algorithm. The theoretical shift necessitates an *ipsative* standardization of geopotential height data prior to conducting PCA.[4] The application of our algorithm involved searching for homogeneous spatial areas within which geopotential height measurements are highly related. Constraints included that independent application of PCA to the S, NS and C samples yields comparable, excellent macro performance (strong eigenvalues) and internal measurement properties across samples, and that mode constituents are physically contiguous. Manually applied to January data the algorithm yielded 46 new modes summarized below (labels are nominal placeholders), ordered by percent of variance explained (i.e., decreasing linearity) for the stationary sample. For Sample, S=stationary, NS=nonstationary, and C=combined S and NS data. M is the number of geopotential height measures (grid locations) constituting the mode.

2155-0182/10/$3.00

Eigen indicates the eigenvalue of the mode for a one-factor PCA solution, and Var is the associated variance explained (100%xEigen/M). The theoretical upper-bound for internal consistency is Alpha=1, and the theoretical lower-bound for root-mean-square-error is RMSR=0. Finally, cumulative total eigenvalue, number of height measures, and total variance explained are also provided across successive modes.

Table 5: Principal Components Analysis of Unconfounded January 500 mb Geopotential Height Data, Separately by Series

							Cumulative Totals		
Mode	Sample	M	Eigen	Var	Alpha	RMSR	Eigen	M	Var
J	S	3	2.866	95.5	.977	.0331	2.866	3	95.5
	NS		2.831	94.4	.970	.0386	2.831		94.4
	C		2.844	94.8	.973	.0364	2.844		94.8
H	S	3	2.840	94.7	.972	.0412	5.706	6	95.1
	NS		2.819	94.0	.968	.0471	5.650		94.2
	C		2.827	94.2	.969	.0445	5.671		94.5
PP	S	3	2.826	94.2	.969	.0360	8.532	9	94.8
	NS		2.641	88.0	.932	.0685	8.291		92.1
	C		2.761	92.0	.957	.0476	8.432		93.7
MM	S	3	2.803	93.4	.965	.0337	11.335	12	94.5
	NS		2.743	91.4	.953	.0433	11.034		92.0
	C		2.773	92.4	.959	.0380	11.205		93.4
P	S	4	3.731	93.3	.976	.0404	15.066	16	94.2
	NS		3.575	89.4	.960	.0608	14.609		91.3
	C		3.651	91.3	.968	.0499	14.856		92.8
L	S	3	2.795	93.2	.963	.0558	17.861	19	94.0
	NS		2.729	91.0	.950	.0735	17.338		91.3
	C		2.790	93.0	.962	.0568	17.646		92.9
NN	S	3	2.793	93.1	.963	.0406	20.654	22	93.9
	NS		2.676	89.2	.939	.0562	20.014		91.0
	C		2.748	91.6	.954	.0464	20.394		92.7
M	S	4	3.724	93.1	.975	.0416	24.378	26	93.8
	NS		3.551	88.8	.958	.0603	23.565		90.6
	C		3.604	90.1	.963	.0575	23.998		92.3
Q	S	3	2.789	93.0	.962	.0541	27.167	29	93.7
	NS		2.613	87.1	.926	.0992	26.178		90.3
	C		2.707	90.2	.946	.0750	26.705		92.1
YY	S	3	2.788	92.9	.962	.0411	29.955	32	93.6
	NS		2.663	88.8	.937	.0566	28.841		90.1
	C		2.729	91.0	.950	.0474	29.434		92.0

2155-0182/10/$3.00

I	S	3	2.785	92.8	.961	.0511	32.740	35	93.5
	NS		2.725	90.8	.950	.0720	31.566		90.2
	C		2.755	91.8	.955	.0612	32.189		92.0
CC	S	3	2.775	92.5	.960	.0492	35.515	38	93.5
	NS		2.653	88.4	.935	.0677	34.219		90.1
	C		2.717	90.6	.948	.0577	34.906		91.9
G	S	3	2.773	92.5	.959	.0586	38.288	41	93.4
	NS		2.802	93.4	.965	.0540	37.021		90.3
	C		2.788	92.9	.962	.0563	37.694		91.9
K	S	3	2.773	92.4	.959	.0561	41.061	44	93.3
	NS		2.672	89.1	.939	.0875	39.693		90.2
	C		2.703	90.1	.945	.0764	40.397		91.8
JJ	S	6	5.544	92.4	.984	.0348	46.605	50	93.2
	NS		5.236	87.3	.971	.0685	44.929		90.0
	C		5.360	89.3	.976	.0568	45.757		91.5
WW	S	3	2.770	92.3	.959	.0547	49.375	53	93.2
	NS		2.675	89.2	.939	.0581	47.604		89.8
	C		2.722	90.7	.949	.0483	48.479		91.5
R	S	3	2.769	92.3	.958	.0617	52.144	56	93.1
	NS		2.869	95.6	.977	.0358	50.473		90.1
	C		2.843	94.8	.972	.0422	51.322		91.6
O	S	3	2.764	92.1	.957	.0646	54.908	59	93.1
	NS		2.864	95.5	.976	.0373	53.337		90.4
	C		2.828	94.2	.970	.0468	54.150		91.8
XX	S	3	2.763	92.1	.957	.0453	57.671	62	93.0
	NS		2.730	91.0	.951	.0498	56.067		90.4
	C		2.744	91.5	.953	.0474	56.894		91.8
T	S	3	2.756	91.9	.956	.0613	60.427	65	93.0
	NS		2.694	89.8	.943	.0801	58.761		90.4
	C		2.715	90.5	.948	.0731	59.609		91.7
F	S	5	4.585	91.7	.977	.0437	65.012	70	92.9
	NS		4.393	87.9	.965	.0742	63.154		90.2
	C		4.471	89.4	.970	.0612	64.080		91.5
EE	S	3	2.749	91.6	.954	.0426	67.761	73	92.8
	NS		2.529	84.3	.907	.0898	65.683		90.0
	C		2.658	88.6	.936	.0608	66.738		91.4
2	S	3	2.743	91.4	.953	.0609	70.504	76	92.8
	NS		2.599	86.6	.923	.0844	68.282		89.8
	C		2.627	87.6	.929	.0824	69.365		91.3
B	S	6	5.472	91.2	.981	.0535	75.976	82	92.7
	NS		5.352	89.2	.976	.0773	73.634		90.0
	C		5.399	90.0	.978	.0654	74.764		91.2

2155-0182/10/$3.00

ZZ	S	3	2.727	90.9	.950	.0464	78.703	85	92.6
	NS		2.787	92.9	.962	.0422	76.421		89.9
	C		2.738	91.3	.952	.0450	77.502		91.2
E	S	4	3.634	90.8	.966	.0511	82.337	89	92.5
	NS		3.526	88.2	.955	.0697	79.947		89.8
	C		3.567	89.2	.960	.0606	81.069		91.1
RR	S	3	2.723	90.8	.949	.0555	85.060	92	92.5
	NS		2.611	87.0	.925	.0813	82.558		89.7
	C		2.658	88.6	.936	.0694	83.727		91.0
D	S	3	2.721	90.7	.949	.0782	87.781	95	92.4
	NS		2.807	93.6	.966	.0521	85.365		89.9
	C		2.724	90.8	.949	.0758	86.451		91.0
C	S	4	3.605	90.1	.964	.0566	91.386	99	92.3
	NS		3.667	91.7	.970	.0500	89.032		89.9
	C		3.637	90.9	.967	.0537	90.088		91.0
U	S	3	2.703	90.1	.945	.0648	94.089	102	92.2
	NS		2.746	91.5	.954	.0624	91.778		90.0
	C		2.727	90.9	.950	.0631	92.815		91.0
LL	S	3	2.695	89.8	.943	.0603	96.784	105	92.2
	NS		2.599	86.6	.923	.0832	94.377		90.0
	C		2.680	89.3	.940	.0646	95.495		90.9
TT	S	3	2.687	89.6	.942	.0565	99.471	108	92.1
	NS		2.840	94.7	.972	.0271	97.217		90.0
	C		2.780	93.3	.964	.0345	98.275		91.0
V	S	3	2.687	89.6	.942	.0845	102.158	111	92.0
	NS		2.659	88.6	.936	.0922	99.876		90.0
	C		2.662	88.7	.937	.0914	100.937		90.9
HH	S	3	2.683	89.4	.941	.0567	104.841	114	92.0
	NS		2.567	85.6	.916	.0994	102.443		89.9
	C		2.615	87.2	.926	.0797	103.552		90.8
UU	S	3	2.681	89.4	.941	.0536	107.522	117	91.9
	NS		2.638	87.9	.931	.0757	105.081		89.8
	C		2.667	88.9	.938	.0623	106.219		90.8
GG	S	3	2.675	89.2	.939	.0627	110.197	120	91.8
	NS		2.723	90.8	.949	.0540	107.804		89.8
	C		2.714	90.5	.947	.0525	108.933		90.8
1	S	3	2.673	89.1	.939	.0603	112.870	123	91.8
	NS		2.771	92.4	.959	.0438	110.575		89.9
	C		2.747	91.6	.954	.0473	111.680		90.8
II	S	3	2.672	89.1	.939	.0578	115.542	126	91.7
	NS		2.745	91.5	.954	.0427	113.320		89.9
	C		2.706	90.2	.946	.0502	114.386		90.8

2155-0182/10/$3.00

DD	**S**	**4**	**3.562**	**89.1**	**.959**	**.0616**	**119.104**	**130**	**91.6**
	NS		**3.540**	**88.5**	**.957**	**.0588**	**116.860**		**89.9**
	C		**3.547**	**88.7**	**.957**	**.0595**	**117.933**		**90.7**
VV	**S**	**3**	**2.656**	**88.5**	**.935**	**.0715**	**121.760**	**133**	**91.5**
	NS		**2.728**	**90.9**	**.950**	**.0479**	**119.588**		**89.9**
	C		**2.717**	**90.6**	**.948**	**.0547**	**120.650**		**90.7**
Y	**S**	**3**	**2.652**	**88.4**	**.934**	**.0941**	**124.412**	**136**	**91.5**
	NS		**2.791**	**93.0**	**.962**	**.0555**	**122.379**		**90.0**
	C		**2.680**	**89.3**	**.940**	**.0864**	**123.330**		**90.7**
3	**S**	**4**	**3.530**	**88.3**	**.956**	**.0733**	**127.942**	**140**	**91.4**
	NS		**3.623**	**90.6**	**.965**	**.0539**	**126.002**		**90.0**
	C		**3.559**	**89.0**	**.959**	**.0671**	**126.889**		**90.6**
FF	**S**	**3**	**2.646**	**88.2**	**.933**	**.0987**	**130.588**	**143**	**91.3**
	NS		**2.701**	**90.0**	**.945**	**.0835**	**128.703**		**90.0**
	C		**2.649**	**88.3**	**.934**	**.0972**	**129.538**		**90.6**
A	**S**	**5**	**4.357**	**87.1**	**.963**	**.0777**	**134.945**	**148**	**91.2**
	NS		**4.538**	**90.8**	**.975**	**.0706**	**133.241**		**90.0**
	C		**4.414**	**88.3**	**.967**	**.0770**	**133.952**		**90.5**
SS	**S**	**3**	**2.603**	**86.8**	**.924**	**.0778**	**137.548**	**151**	**91.1**
	NS		**2.755**	**91.8**	**.955**	**.0471**	**135.996**		**90.1**
	C		**2.652**	**88.4**	**.934**	**.0676**	**136.604**		**90.5**
BB	**S**	**4**	**3.473**	**86.8**	**.949**	**.0656**	**141.021**	**155**	**91.0**
	NS		**3.612**	**90.3**	**.964**	**.0566**	**139.608**		**90.1**
	C		**3.514**	**87.8**	**.954**	**.0645**	**140.118**		**90.4**

There is no evidence of paradoxical confounding (performance results for C always fall between results for S and NS), and the percentage of variance explained, Alpha, and RMSR meet psychometric criteria for “good to excellent” fit for exploratory PCA models.[1,3] We also examined internal measurement properties of the individual modes via one-factor PCA of the three sample scores (S, NS, C), and analysis revealed virtually perfect measurement: for every mode, percent of total variance (of M measures) explained > 99.9%; Alpha > 0.99, and RMSR $\leq$ 0.0002. We attempted to model the original ten modes using the new 46 modes, and vice versa, using multiple regression analysis, but no satisfactory models were identified: the original ten modes and the new 46 modes are *not* related to each other.

Considered together these findings clearly show that the 46 new and unique modes eliminate every *empirical* problem identified for the original ten modes: there is no evidence of Simpson’s paradox (S and NS data may be combined without inducing confounding); model performance and phenomenon effect strength are not erroneously misestimated (estimates from all samples are convergent); and mode scores exhibit ideal measurement properties. The new modes also address all *theoretical* concerns identified for the original ten modes: granularity increased 4.6-fold; the new modes

2155-0182/10/$3.00

are parsimonious (factor weighting coefficients are all approximately one in absolute magnitude, each grid location appears on only one mode); mode scores are sensitive (composed of six or fewer strongly related grid locations, small changes in geopotential heights are easily detectable); and the modes are extremely well modeled by PCA, representing a set of nearly perfectly linear measures.

Qualitative Interpretation of Ipsative Modes

Figure 4 locates the ipsative modes on a polar projection map of the northern hemisphere.

Figure 4: Polar projection Map of the Ipsative Modes

2155-0182/10/$3.00

The principal-component-derived CPC modes of upper-air variability listed in Table 2 are highly consistent with the modes identified in the original principal components analysis[2] of 700 mb height data, and have counterparts in the ipsative modes developed presently.

The first mode, North Atlantic Oscillation (NAO), had strong positive coefficients for grid points over Greenland, corresponding to ipsative mode U. NAO also had strong negative coefficients for grid points in the North Atlantic, west of the Azores (ipsative mode VV); Manchuria (ipsative mode H); and the central plains of the US (between ipsative factors EE and 1).

The second mode, East Atlantic Pattern (EA), had strong positive coefficients for grid points over North Africa (ipsative mode DD), and in the Atlantic east of Cuba (ipsative mode F). EA also had strong negative coefficients for grid points in the North Atlantic, east of Labrador and south of Greenland (ipsative mode FF).

The West Pacific Pattern (WP) had strong positive coefficients for grid points in the Philippine Sea (ipsative mode D), and strong negative coefficients for grid points just east of Kamchatka (ipsative mode ZZ).

The East Pacific/North Pacific Pattern (EP/NP) had strong positive coefficients for grid points over southeast Alaska (between ipsative modes GG and 2). EP/NP also had strong negative coefficients for grid points in the North Pacific south of the Aleutian Islands (ipsative mode TT), and near James Bay in Canada (ipsative mode M).

The Pacific/North American Pattern (PNA) had strong positive coefficients for grid points west of Hawaii (ipsative mode A), and in the Pacific Northwest of the US (ipsative mode LL). PNA also had strong negative coefficients for grid points in the North Pacific southwest of the Aleutian Islands (ipsative mode O), and over the southeast US (ipsative mode EE).

The East Atlantic/West Russia Pattern (EA/WR) had strong positive coefficients for grid points near England (between ipsative factors II and UU), and in Siberia north of Manchuria (ipsative mode G). EA/WR also had strong negative coefficients for grid points northeast of the Caspian Sea (ipsative mode JJ).

The Scandinavian Pattern (SCA) had strong positive coefficients for grid points in Central Russia (between ipsative modes G and P), and in the North Atlantic, northwest of Spain (ipsative mode WW). SCA also had strong negative coefficients for grid points near Finland (between ipsative modes XX and JJ).

The Tropical/Northern Hemisphere Pattern (TNH) had strong positive coefficients for grid points in the North Pacific west of the Pacific Northwest of the US (ipsative mode SS), and near the Bahamas (ipsative mode MM). TNH also had strong negative coefficients for grid points near James Bay in Canada (ipsative mode M).

The Polar/Eurasia Pattern (POL) had strong positive coefficients for grid points in eastern Mongolia (near ipsative modes G and H), and strong negative coefficients for grid points in the Arctic Ocean north of eastern Siberia (ipsative mode HH).

Finally, the Pacific Transition Pattern (PT)—which did not materialize in either of the original principal component analyses for the month of January, had for the month of September strong positive coefficients for grid points over the northern plains of the US (ipsative mode 1), and west of Hawaii (ipsative mode A). PT also had strong negative coefficients for grid points in the North Pacific south of Alaska (ipsative mode C), and over the eastern US (ipsative mode V).

Predicting Temperature Anomalies

To determine whether predictive validity is augmented by nonconfounded measurement, we assessed whether statistical models that use the 46 newly discovered (*vs*. original ten) modes of northern hemisphere upper-air variability produce more accurate temperature forecasting.

2155-0182/10/$3.00

We used classification tree analysis, or CTA[5], to predict whether mean temperature in January, February, and March fell above or below the median temperature for the years 1950-2007, for 48 contiguous US states. Falling within the optimal data analysis paradigm, CTA explicitly maximizes model accuracy when applied to a given sample or series.[6] Proprietary software was used to automatically identify CTA models that weighted more heavily observations having greater deviations from the median temperature: of course, depending on the application, "natural weights" such as inches of rain, may be used instead of, or in conjunction with, "tailored weights" such as we used.[6] The weighted CTA algorithm was performed using three sets of attributes: *ipsative modes* (46 modes discovered presently); *published normative modes* obtained from the CPC, with PT omitted due to inactivity in January; and *computed normative modes* obtained from our replication of the CPC analysis using only January data.

The findings of these analyses are summarized in Table 6. Tabled are modes (see Table 5 for coding) emerging with $p<0.05$ in the weighted CTA model. The weights were determined by sorting the observations by monthly mean temperature, and adding 1.5 for every position above or below the median. WESS is a standardized measure of weighted effect strength, on which 0 is the level of weighted predictive accuracy that is expected by chance, and 100 represents errorless (perfect) weighted predictive accuracy.[6] A dash (-) indicates no solution was identified having $p<0.05$ for any mode; a missing row indicates no solution was identified for any data type (ipsative, published, or computed); and an asterisk (*) indicates that results for the indicated modes were identical to findings for the ipsative modes.

Models derived using ipsative modes to predict temperature anomalies in the United States convincingly and broadly outperformed corresponding models derived with normative modes, when considered from the perspective of predictive accuracy, and quantified using the standardized WESS metric:

- For a given state and month (corresponding to individual rows in Table 6), the ipsative mode model yielded the greatest WESS 117 times (91.4%), versus 5 and 6 (3.9% and 4.7%) times for published and computed normative mode models, respectively.

- In January the ipsative mode models always achieved greater WESS than the corresponding normative mode models. In February the ipsative mode models almost always (93.2% of the time) achieved greatest WESS (44 states had models based on February data), and even as the data aged substantially—for March, ipsative models usually (78.1% of the time) achieved greatest WESS (32 states had models using March data).

- For January data, using ipsative modes, all 48 states had CTA models with WESS$\geq$90%, versus two states with CTA models involving published normative modes, and one state CTA model involving computed normative modes. For February data, using ipsative modes, a dozen states had CTA models with WESS$\geq$90% (and three for March data), versus none using normative modes.

2155-0182/10/$3.00

Table 6: Temperature Prediction via Weighted CTA by US State, for January, February, and March of 2008, Using Ipsative mode Scores, and Published and Computed Raw Mode Scores

State	Month	Ipsative Modes	WESS	Published Normative Modes	WESS	Computed Normative Modes	WESS
Alabama	Jan	B,EE,JJ,MM,2	97.43	EAWR,NAO,PNA	71.30	2,3,9	68.44
	Feb	A,C,I,EE,PP	93.80	NAO,SCA	57.74	3,6	62.59
	Mar	DD,GG	51.55	-	-	-	-
Arkansas	Jan	C,R,EE,MM,XX,2	98.54	EPNP,PNA,WP	74.63	3,5,8	80.36
	Feb	CC,DD,RR,VV	88.90	EPNP,NAO	63.35	3,5,10	79.31
	Mar	II	38.63	-	-	-	-
Arizona	Jan	C,H,U,YY,1	93.22	NAO,POL,WP	75.80	2,6	84.40
	Feb	F,II,PP	72.65	-	-	-	-
California	Jan	C,BB,GG,VV,WW,YY	98.89	PNA,WP	52.83	2,6	77.79
	Feb	RR,TT	74.87	EAWR,EPNP,PNA	76.04	-	-
Colorado	Jan	I,V,T,SS,WW	95.62	-	-	2,6	79.60
	Feb	M,O,P,Q,BB,3	91.70	-	-	-	-
	Mar	J,SS,1	72.76	NAO	39.74	1,5	57.69
Connecticut	Jan	E,K,LL,2	96.43	EA,EAWR,EPNP,NAO,WP	86.62	3,4,5	74.52
	Feb	PP,2	50.44	-	-	-	-
Delaware	Jan	V,EE,MM,2	95.15	EAWR,EPNP,NAO,WP	84.63	3,5,7	71.71
	Feb	HH,JJ,PP,SS	73.41	NAO	42.84	3	44.89
	Mar	J	37.97	-	-	-	-

Florida	Jan	A,G,O,MM,PP,YY	98.95	EAWR,EPNP,PNA	89.19	2,3,6	82.23
	Feb	D,Q,CC,LL,RR	93.22	NAO	40.50	5	63.06
	Mar	K,DD,EE,GG	75.80	-	-	-	-
Georgia	Jan	P,EE,MM,PP,2	98.13	EAWR,EPNP,PNA	84.04	2,3,9	70.66
	Feb	A,C,H,EE,PP	92.34	NAO,SCA	57.16	3,5	73.47
Iowa	Jan	H,L,V,2	93.51	EPNP,SCA,WP	76.74	3,4,7,8	84.57
	Feb	D,DD,JJ	80.95	EAWR	49.09	3,7	44.18
	Mar	J,HH,LL,PP,1	87.26	PNA	41.15	-	-
Idaho	Jan	C,I,MM,SS,ZZ	94.56	-	-	2,3,6	81.59
	Feb	D,Q,R,BB	86.91	PNA	60.78	-	-
	Mar	D,R,Y,RR	93.86	NAO,PNA,SCA	83.99	1,5	63.82
Illinois	Jan	B,D,E,V,EE,WW,2	99.36	EPNP,PNA,WP	83.52	3,4,8	86.62
	Feb	D,DD,GG,PP	83.40	EAWR,NAO,SCA	66.04	-	-
	Mar	-	-	PNA	39.86	-	-
Indiana	Jan	D,E,K,V,EE,WW	96.61	EPNP,PNA,WP	82.70	3,5,8	82.35
	Feb	K,U,NN,RR	71.01	EAWR,NAO,POL	73.58	3	40.44
	Mar	L,II	57.04	PNA	39.39	1,10	57.22
Kansas	Jan	F,Q,GG,WW,1	96.73	EPNP,WP	59.44	1,3,6,9	69.43
	Feb	V,CC,FF,UU	80.19	EAWR,NAO	60.55	3,6,7,9	82.82
	Mar	D,H,FF	73.00	-	-	-	-

2155-0182/10/$3.00

Kentucky	**Jan**	**E,J,V,PP,2**	**96.20**	**EAWR,EPNP,NAO**	**79.37**	**3,5**	**73.82**
	Feb	**F,I,Q,U,RR**	**96.55**	**NAO**	**53.36**	**3,6**	**60.14**
Louisiana	**Jan**	**U,V,EE,LL,3**	**96.20**	**NAO,PNA**	**69.37**	**1,2,6**	**84.22**
	Feb	**A,C,EE,PP**	**79.37**	**NAO**	**53.71**	**3,5,6,10**	**79.19**
	Mar	**D,DD**	**52.95**	**-**	**-**	**-**	**-**
Massachusetts	**Jan**	**E,I,K,LL,2**	**97.72**	**EA,EAWR,EPNP,NAO,WP**	**90.06**	**3,4,5**	**73.70**
	Mar	**-**	**-**	**-**	**-**	**2**	**38.92**
Maryland	**Jan**	**E,G,L,V,RR,UU**	**98.54**	**EAWR,EPNP,WP**	**84.28**	**3,5,8**	**71.30**
	Feb	**Y,RR,XX**	**69.96**	**NAO,POL**	**55.00**	**3**	**46.41**
Maine	**Jan**	**E,O,LL,2**	**95.21**	**EPNP,WP**	**61.60**	**3,8**	**65.81**
	Feb	**Q,RR,1**	**76.04**	**-**	**-**	**7**	**39.63**
	Mar	**Q**	**39.10**	**-**	**-**	**-**	**-**
Michigan	**Jan**	**D,E,GG,II**	**97.37**	**EAWR,EPNP,WP**	**81.71**	**3,5,7,8**	**86.56**
	Feb	**I,DD,GG,HH**	**82.76**	**EAWR,NAO**	**53.65**	**3,7**	**51.43**
	Mar	**J,L**	**57.51**	**PNA,SCA**	**59.73**	**2**	**44.18**
Minnesota	**Jan**	**C,E,CC,1,2**	**95.73**	**EAWR,EPNP,PNA,WP**	**88.49**	**4,5,8**	**79.78**
	Feb	**F,Q,NN,RR**	**78.08**	**EAWR**	**44.71**	**7,10**	**61.19**
	Mar	**J,O,1**	**82.70**	**PNA,WP**	**56.81**	**2**	**40.68**
Missouri	**Jan**	**D,E,F,EE,GG**	**94.92**	**EPNP,PNA,WP**	**85.74**	**3,4,7,8**	**93.98**
	Feb	**EE,RR,SS,TT,VV**	**93.44**	**EAWR,EPNP,NAO,POL**	**77.93**	**3,5,7**	**76.52**

2155-0182/10/$3.00

Mississippi	Jan	I,V,EE,2	96.20	EPNP,NAO,PNA	86.91	1,2,6	78.73
	Feb	A,C,EE,PP	79.54	NAO	52.78	3,6,10	71.95
	Mar	DD,GG	51.32	-	-	-	-
Montana	Jan	E,F,L,ZZ,2	96.67	EPNP,PNA,SCA,WP	84.04	2,6,9	75.45
	Feb	A,G,Q,R	85.62	PNA	47.05	7	49.80
	Mar	CC,GG,TT,3	80.60	PNA	45.35	1	39.22
North Carolina	Jan	E,Y,MM,XX	95.38	EAWR,EPNP,PNA	86.15	3,5	71.60
	Feb	D,T,Y,RR,VV	89.83	NAO,SCA	54.94	3,9	56.52
North Dakota	Jan	C,E,L,WW	96.90	EPNP,PNA,SCA,WP	91.41	1,3,5,7	80.89
	Feb	D,Q,II,RR	94.21	EAWR,PNA	61.84	7	45.35
	Mar	J,GG,1	77.91	PNA	43.83	-	-
Nebraska	Jan	A,V,DD,1,2	95.56	EPNP,WP	57.10	1,3,9	70.19
	Feb	Q,DD,RR,TT	86.44	EAWR	43.83	-	-
	Mar	D,LL	74.81	-	-	-	-
New Hampshire	Jan	E,K,JJ,LL,2	97.49	EA,EPNP,WP	71.89	3,5,7	70.72
	Feb	-	-	-	-	7	39.28
	Mar	-	-	-	-	2	40.56
New Jersey	Jan	E,K,H,LL	98.48	EA,EAWR,EPNP,NAO,WP	87.38	3,4,5	76.74
	Feb	Y,RR,1	70.72	-	-	3	40.68

2155-0182/10/$3.00

New Mexico	**Jan**	**G,T,RR,UU,ZZ**	**97.84**	**EA,NAO**	**64.64**	**1,6**	**84.16**
	Feb	**F,G,RR,VV,1**	**88.43**	**NAO**	**43.25**	**6**	**42.84**
	Mar	**G,Y,3**	**73.52**	**-**	**-**	**-**	**-**
Nevada	**Jan**	**C,I,V,SS,ZZ**	**96.43**	**-**	**-**	**2,3,6**	**86.62**
	Feb	**RR,TT,WW**	**76.62**	**EA,PNA**	**60.43**	**-**	**-**
	Mar	**1**	**38.81**	**NAO**	**41.44**	**-**	**-**
New York	**Jan**	**II,MM,XX,2**	**97.02**	**EA,EAWR,EPNP,NAO,WP**	**89.42**	**3,4,5**	**77.79**
	Mar	**L**	**38.98**	**-**	**-**	**-**	**-**
Ohio	**Jan**	**E,L,V,RR**	**96.67**	**EAWR,EPNP,WP**	**80.65**	**3,5,8**	**79.43**
	Feb	**D,GG,HH,PP**	**81.71**	**NAO,POL**	**59.03**	**3**	**39.98**
	Mar	**L,II**	**56.22**	**-**	**-**	**1,10**	**55.93**
Oklahoma	**Jan**	**F,K,Q,DD,E,2**	**96.90**	**EA,EPNP**	**59.15**	**8**	**63.35**
	Feb	**H,EE,RR,TT,VV**	**85.86**	**EPNP,NAO**	**67.15**	**3,6,7**	**74.17**
	Mar	**D,J**	**49.09**	**-**	**-**	**-**	**-**
Oregon	**Jan**	**C,I,EE,MM,PP**	**91.88**	**NAO,PNA,WP**	**83.99**	**2,3,5**	**81.18**
	Feb	**Q,R,NN,3**	**86.15**	**PNA**	**61.72**	**1,3,7**	**63.35**
	Mar	**F,R,V,SS,2**	**82.58**	**NAO,PNA,POL**	**69.08**	**-**	**-**
Pennsylvania	**Jan**	**E,J,HH,YY**	**96.96**	**EAWR,EPNP,NAO,WP**	**85.80**	**3,5,8**	**72.36**
	Feb	**Q,RR**	**58.45**	**NAO**	**43.42**	**3,7**	**56.81**
	Mar	**L**	**39.80**	**-**	**-**	**-**	**-**

2155-0182/10/$3.00

Rhode Island	**Jan**	**E,K,LL,2**	**96.84**	**EA,EAWR,EPNP,NAO,WP**	**86.50**	**3,4,5**	**75.34**
	Feb	**G,K,2**	**73.52**	**-**	**-**	**-**	**-**
	Mar	**J,Q,CC,EE,XX**	**71.54**	**-**	**-**	**-**	**-**
South Carolina	**Jan**	**Q,R,MM,RR**	**96.73**	**EAWR,EPNP,PNA**	**85.91**	**2,3,9**	**70.89**
	Feb	**D,Q,JJ,RR**	**90.01**	**NAO,SCA**	**55.29**	**3,6**	**62.01**
South Dakota	**Jan**	**C,E,L,2**	**97.25**	**EPNP,SCA,WP**	**88.02**	**5,8**	**62.30**
	Feb	**D,Q,II,RR**	**92.69**	**EAWR**	**47.69**	**7**	**42.20**
	Mar	**D,J,DD,1**	**87.67**	**-**	**-**	**-**	**-**
Tennessee	**Jan**	**I,Q,V,EE,3**	**94.86**	**EAWR,EPNP,NAO,PNA**	**77.85**	**3,5**	**69.02**
	Feb	**D,T,U,RR,TT**	**87.38**	**NAO**	**53.13**	**3,6**	**56.75**
Texas	**Jan**	**C,EE,GG,NN,RR**	**92.17**	**NAO,PNA,POL**	**68.73**	**1,2,6**	**82.99**
	Feb	**A,M,JJ,RR,WW,3**	**94.62**	**NAO**	**51.96**	**3,5,10**	**74.34**
	Mar	**Y,FF,LL,PP**	**72.36**	**-**	**-**	**-**	**-**
Utah	**Jan**	**C,I,V,BB,SS,ZZ**	**96.32**	**-**	**-**	**1,2,6**	**84.34**
	Feb	**Q,CC,DD,NN**	**80.25**	**PNA**	**44.59**	**-**	**-**
	Mar	**1**	**41.61**	**NAO**	**43.13**	**1,5**	**58.62**
Virginia	**Jan**	**E,H,L,V,RR**	**97.37**	**EAWR,EPNP,PNA**	**85.68**	**3,5**	**72.06**
	Feb	**A,H,Y,RR,VV**	**92.87**	**NAO**	**49.50**	**3,5,9**	**56.98**
Vermont	**Jan**	**E,CC,JJ,LL,2**	**99.12**	**EA,EPNP,NAO,WP**	**73.41**	**3,5,7**	**71.30**
	Mar	**Q**	**42.72**	**-**	**-**	**-**	**-**

2155-0182/10/$3.00

Washington	**Jan**	**L,O,CC,EE,VV**	**97.78**	**EA,NAO,PNA,WP**	**91.06**	**2,5,6**	**76.68**
	Feb	**M,R,EE,WW**	**88.37**	**PNA**	**67.45**	**1,7**	**58.56**
	Mar	**D,H,PP,TT,XX,2**	**92.93**	**PNA**	**57.39**	**-**	**-**
Wisconsin	**Jan**	**E,M,GG,UU,ZZ**	**97.84**	**EAWR,EPNP,PNA**	**79.31**	**3,5,8**	**75.04**
	Feb	**Q,RR,ZZ,1**	**74.87**	**EAWR**	**44.54**	**7**	**48.39**
	Mar	**L,T,CC,GG,NN**	**93.10**	**PNA,SCA**	**65.81**	**2**	**43.60**
West Virginia	**Jan**	**E,H,V,EE,LL**	**98.19**	**EAWR,EPNP,PNA,SCA**	**83.46**	**3,5**	**76.74**
	Feb	**D,T,U,LL,RR,TT**	**95.91**	**NAO**	**52.54**	**3**	**42.31**
Wyoming	**Jan**	**K,DD,MM,YY,ZZ**	**92.11**	**-**	**-**	**2,3,5**	**77.50**
	Feb	**C,G,Q,DD**	**84.57**	**-**	**-**	**-**	**-**
	Mar	**D,F,LL,SS**	**89.89**	**NAO**	**43.37**	**1**	**41.03**

2155-0182/10/$3.00

- We statistically contrasted the WESS of each pair of these three sets of factors. If no model was found, WESS was assumed to be zero. ODA was used to determine which set of modes was better at predicting whether or not the mean temperature of the states exceeded the median. The PTMP procedure[7] was used to estimate the exact Type I error of each contrast. Analyses indicated that ipsative mode models had significantly greater WESS than the published or computed normative mode models for all three months (p's <0.0001), and that normative models could *never* reliably be discriminated from each other by WESS (p's>0.17).

- As a test of cross-sample generalizability we also evaluated a larger field of northern hemisphere data. In the crutem3v dataset are 217 locations which have no missing data for January, February or March, for the years 1948-2007. As a test of cross-method generalizability, temperature predictions for each location and month were obtained using stepwise multiple regression analysis: the independent variables were the January data, and ipsative, published raw, or computed raw modes were used as dependent variables. The R^2 value for each model was determined: if no model was found, R^2 was assumed to be zero. Statistical comparison via the PTMP procedure showed that ipsative modes clearly outperformed the other modes (p's<0.0001). Computed raw modes outperformed published raw modes in all cases: contrasts were statistically significant for January and February (p's<0.0001), but not March (p<0.27).

Predicting Precipitation Anomalies

As a second investigation of predictive validity we assessed whether statistical models that use the ipsative modes produce more accurate precipitation forecasting. We used CTA to predict whether mean precipitation in January, February, and March fell above or below the median precipitation for the years 1950-2007, for 48 contiguous US states. As for temperature modeling, the weighted CTA algorithm was performed using three sets of attributes: the 46 newly discovered ipsative modes; published normative modes (obtained from the CPC, with PT omitted due to inactivity in January); and computed normative modes (obtained from our replication of CPC analysis using only January data). The findings of these analyses are summarized in Table 7. Tabled are modes (see Table 5 for coding) emerging with p<0.05 in the weighted CTA model. The weights were determined by the same method as was used in predicting temperature anomalies, but total monthly precipitation was used for the sort and median.

As when modeling temperature anomalies, models derived using ipsative modes to predict precipitation anomalies in the United States convincingly and broadly outperformed corresponding models derived by normative modes, when considered from the perspective of predictive accuracy:

- For a given state and month (corresponding to individual rows in Table 7), the ipsative mode model yielded the greatest WESS 126 times (92.6%), versus 5 (3.7%) times each for the published and computed normative mode models.

2155-0182/10/$3.00

Table 7: Precipitation Prediction via Weighted CTA by US State, for January, February, and March of 2008, Using Ipsative mode Scores, and Published and Computed Raw Mode Scores

State	Month	Ipsative Modes	WESS	Published Normative Modes	WESS	Computed Normative Modes	WESS
Alabama	Jan	C,O,P,MM,NN	89.01	EA,SCA	64.47	8	39.86
	Feb	A,R,T,V,II	87.03	EA	39.45	-	-
	Mar	I,YY	59.56	-	-	-	-
Arkansas	Jan	C,R,FF,MM,YY	90.01	NAO,PNA	76.27	1,3,9	80.54
	Feb	Q	39.98	-	-	-	-
	Mar	HH	39.28	-	-	-	-
Arizona	Jan	G,LL,SS	73.47	EPNP	39.63	9	52.02
	Feb	I,J,L,1	87.14	EPNP,SCA	62.83	3,5	71.36
	Mar	G,Q,T,JJ,SS	84.51	PNA	38.11	5,7,9	57.10
California	Jan	BB,LL,NN,SS,2	94.62	EA	48.92	3,6,8	76.33
	Feb	V,SS,XX	68.79	-	-	-	-
	Mar	C,R,U,SS	84.57	NAO	44.07	-	-
Colorado	Jan	D,EE	59.44	PNA	52.48	-	-
	Feb	NN,XX	65.75	SCA	45.59	3,7	59.73
	Mar	II,SS,3	76.21	PNA	45.47	-	-
Connecticut	Jan	V,BB,XX	87.67	-	-	5	42.02
	Feb	P,HH	77.26	EAWR	43.54	10	38.92
	Mar	G,H,J	51.32	POL	44.07	-	-

2155-0182/10/$3.00

Delaware	Jan	B,RR	57.74	EAWR,NAO	51.49	2	41.44
	Feb	C,BB,EE	70.31	-	-	6	46.29
	Mar	CC,DD,EE,PP	90.77	NAO,WP	55.35	-	-
Florida	Jan	F,O,BB,CC,DD	92.11	EA	43.66	3	40.62
	Feb	T,EE,VV,2	94.62	-	-	-	-
	Mar	C,D,O,SS,TT	89.60	-	-	4,5	53.54
Georgia	Jan	O,MM,NN	73.76	EA	68.32	6,8	57.63
	Feb	C,J,T,SS,WW	91.88	-	-	3	42.02
Iowa	Jan	GG,NN	59.38	EAWR,PNA	60.61	1	49.68
	Feb	G,I,R,PP	77.97	-	-	-	-
	Mar	T,EE	56.52	-	-	-	-
Idaho	Jan	E,L,T,GG,WW,1	98.48	EPNP,PNA,SCA	75.75	1,6,8,9	86.50
	Feb	J,M,U,NN,XX	85.86	EA,POL	64.52	5,7	62.77
	Mar	I,U,HH,LL,3	89.54	EA,NAO,WP	80.77	2,4,5	84.80
Illinois	Jan	H,Q,R,MM,NN	92.99	PNA	50.32	9	46.05
	Feb	Q,U,BB,HH	81.06	-	-	7	39.51
	Mar	E,J,JJ,UU	87.90	-	-	-	-
Indiana	Jan	F,I,EE,HH,PP	91.23	NAO,PNA	72.59	9	40.56
	Feb	R,EE,LL,XX	83.46	-	-	4,7	66.45
	Mar	O,JJ,SS	74.05	-	-	-	-

2155-0182/10/$3.00

Kansas	**Jan**	**E,Y,GG,LL**	**84.72**	**-**	**-**	**3,6**	**55.91**
	Feb	**F,K,M,FF**	**78.08**	**-**	**-**	**-**	**-**
	Mar	**D,H,R,2**	**81.12**	**PNA**	**41.55**	**-**	**-**
Kentucky	**Jan**	**A,V,HH,PP**	**89.42**	**PNA,SCA**	**69.67**	**1,6**	**79.95**
	Feb	**Q,V,II,LL,TT**	**86.09**	**-**	**-**	**7**	**50.96**
	Mar	**G,NN,XX**	**75.39**	**-**	**-**	**2**	**53.83**
Louisiana	**Jan**	**H,DD,FF,WW**	**80.77**	**EA,EPNP**	**51.61**	**-**	**-**
	Feb	**C,P,T**	**71.24**	**-**	**-**	**2**	**40.09**
	Mar	**A,E,K,FF,WW**	**85.80**	**-**	**-**	**6,7**	**64.87**
Massachusetts	**Jan**	**-**	**-**	**-**	**-**	**2**	**39.45**
	Feb	**I,SS,WW,1**	**78.43**	**-**	**-**	**-**	**-**
	Mar	**C,G,HH**	**66.74**	**POL**	**50.85**	**-**	**-**
Maryland	**Jan**	**G,H,WW**	**69.73**	**-**	**-**	**-**	**-**
	Feb	**E,P,Q,YY**	**88.54**	**-**	**-**	**6**	**42.96**
	Mar	**I,HH,RR,VV**	**94.80**	**SCA,WP**	**53.19**	**-**	**-**
Maine	**Jan**	**HH,WW,YY,2**	**86.44**	**-**	**-**	**5**	**39.22**
	Feb	**J,NN,WW**	**70.25**	**-**	**-**	**1,5**	**65.40**
	Mar	**I,J,HH,SS,1**	**86.85**	**POL**	**43.78**	**-**	**-**
Michigan	**Jan**	**H,Q,T,GG,MM**	**86.97**	**PNA**	**50.38**	**1,6**	**53.95**
	Feb	**D,DD**	**68.26**	**-**	**-**	**-**	**-**

2155-0182/10/$3.00

Minnesota	Jan	P,FF,GG	77.62	-	-	-	-
	Mar	Q,YY,3	78.43	-	-	-	-
Missouri	Jan	O,Q,R,EE,SS	89.77	PNA	51.55	2,3,8	72.88
	Feb	Q,U	58.85	-	-	-	-
	Mar	L,JJ	62.77	-	-	-	-
Mississippi	Jan	U,V,MM,XX	91.12	EAWR	40.50	-	-
	Feb	J,NN	48.51	-	-	-	-
	Mar	CC,FF,2	73.12	-	-	-	-
Montana	Jan	L,V,FF,GG,VV	96.90	PNA	60.08	2,3,5,6	83.23
	Feb	M,O,P,BB	89.13	EAWR,PNA,POL	76.97	2,7	71.83
	Mar	B,H,M,Q,TT	85.62	-	-	-	-
North Carolina	Jan	MM	41.15	WP	38.98	-	-
	Feb	F,L,R,PP,YY	84.40	-	-	-	-
	Mar	G,EE,PP	73.41	-	-	-	-
North Dakota	Jan	C,D,L,HH	83.34	PNA	46.70	-	-
	Feb	L,NN,WW	61.72	-	-	-	-
	Mar	I	45.35	-	-	-	-
Nebraska	Jan	Q,EE,PP	75.86	-	-	9	39.98
	Feb	M,V,WW,XX	84.34	SCA	39.28	8,10	52.02
	Mar	FF,MM,NN	73.70	PNA	44.77	-	-

2155-0182/10/$3.00

New Hampshire	Jan	Q,HH,WW,2	86.44	-	-	5	46.23
	Feb	NN,WW,2	70.89	-	-	-	-
	Mar	H,R,P,HH	85.74	POL	48.57	-	-
New Jersey	Feb	E,P,U,JJ	77.32	EAWR	40.68	-	-
	Mar	J,P,JJ,2	76.50	POL,SCA	56.52	-	-
New Mexico	Jan	O,EE,GG,LL	89.17	-	-	9	46.72
	Feb	A,O,EE,RR,WW	78.08	-	-	3,6	51.96
	Mar	Q,GG,SS	80.19	NAO,PNA	54.88	1,7	55.52
Nevada	Jan	U,LL,SS,YY	89.01	-	-	1	47.34
	Feb	V,DD,RR,SS,XX	92.69	-	-	-	-
	Mar	C,G,U,SS	72.82	EA,NAO	58.09	-	-
New York	Mar	D,H,R,HH,NN	87.90	EPNP	40.39	-	-
Ohio	Jan	U,BB,HH,MM	77.85	NAO,PNA,WP	75.39	1,6	60.08
	Feb	F,P,R,TT	95.79	EAWR	39.45	7	54.24
	Mar	I,SS	62.83	-	-	2,9	55.29
Oklahoma	Jan	D,L,EE,FF,UU	90.88	WP	40.68	6,9	68.73
	Feb	YY	41.03	-	-	1,6	61.48
	Mar	D,H,Q,II	86.85	-	-	2,5	62.77
Oregon	Jan	D,GG,LL,XX,YY	99.59	EPNP,PNA,SCA	78.61	1,6,8,9	89.66
	Feb	P,LL,3	72.36	EA,POL	74.28	6	45.18
	Mar	I,V,FF	76.91	EA,NAO	52.54	2	44.54

2155-0182/10/$3.00

Pennsylvania	Jan	J,P,U,MM	69.14	-	-	-	-
	Feb	E,Q,II,TT,WW	90.24	EAWR	40.56	2,7	52.07
	Mar	J,O,SS,XX	79.84	-	-	3	39.86
Rhode Island	Jan	JJ,LL,NN,UU	83.11	-	-	-	-
	Feb	E,P,U	86.15	EAWR	42.14	-	-
	Mar	CC	39.63	EA,POL	71.60	5,9	53.42
South Carolina	Jan	T,JJ	67.45	EA,WP	74.40	6,8	54.59
	Feb	L,R,CC,PP	75.69	-	-	-	-
South Dakota	Jan	Q,FF,TT	76.10	-	-	-	-
	Feb	A,U,LL,ZZ	87.90	-	-	-	-
	Mar	A,H,GG,WW	76.10	-	-	5,10	63.30
Tennessee	Jan	E,P,V,HH,ZZ	90.65	PNA	68.44	1,2,6	80.42
	Mar	I,M	58.27	-	-	2	42.02
Texas	Jan	L,JJ	65.81	EAWR,POL,SCA	50.15	1,6,7,9	88.90
	Feb	F,V,SS,TT,ZZ	89.95	-	-	3,7	59.15
	Mar	D,J,R,XX,2	87.61	-	-	5,7,9	77.56
Utah	Jan	J,SS,XX	77.32	PNA	40.04	1	43.13
	Feb	B,F,M,DD,XX	91.93	-	-	3	49.56
	Mar	NN,SS,WW	73.47	NAO	40.33	2	39.45
Virginia	Jan	G,I	71.71	-	-	-	-
	Feb	C,Q,NN	79.31	EA	40.09	6,8	71.42
	Mar	F,K,CC,MM,PP,RR	96.08	-	-	-	-

2155-0182/10/$3.00

Vermont	Jan	H,Q,V	77.15	-	-	5	49.74
	Feb	C,J,K,M,FF	87.03	-	-	-	-
	Mar	J	40.74	EPNP,WP	60.43	-	-
Washington	Jan	J,GG,NN,2	90.65	EA,EAWR	52.78	1,9	57.10
	Feb	-	-	EA,POL	54.35	5,6	61.84
	Mar	I,FF	55.58	EA	45.06	2,10	60.90
Wisconsin	Jan	A,MM,PP	76.97	PNA	47.63	1	48.39
	Feb	G,J,P,R	85.33	-	-	1,7	59.61
	Mar	Q,R,YY,1	83.69	-	-	-	-
West Virginia	Jan	HH,MM,3	81.94	EA,NAO,PNA	73.64	1,6,8	70.72
	Feb	A,C,Q,R	81.77	-	-	-	-
	Mar	D,G,L,M,JJ	94.16	SCA	38.63	2	41.26
Wyoming	Jan	T,YY,1	85.86	EA,PNA,SCA,WP	79.60	2,9	59.91
	Feb	CC,JJ,RR,WW	74.40	SCA	39.22	-	-
	Mar	D,G,BB,HH,TT	86.09	-	-	6	41.67

2155-0182/10/$3.00

- In January, ipsative mode models achieved greater WESS than corresponding normative mode models 91.3% of the time (46 states had models based on January data). Similarly, in February the ipsative mode models almost always (93.3% of the time) achieved greatest WESS (45 states had models based on February data), and even as data aged substantially—in March, ipsative models almost always (93.5% of the time) achieved greatest WESS (46 states had models based on March data).

- Using ipsative modes, for January data 12 states had CTA models with WESS$\geq$ 90%, as did 6 states for February data and 4 states for March data. Zero normative mode models achieved this level of WESS in any month modeled.

- We statistically contrasted the WESS of each pair of these three sets of modes. If no model was found, then WESS was assumed to be zero. We used ODA to determine which set of modes was better at predicting whether the mean precipitation of the states exceeded the median, or not. The PTMP procedure[7] was used to estimate the exact Type I error for each contrast. Analyses of January data (March and February had comparatively sparse data) indicated that the ipsative mode model had significantly greater WESS than the normative mode models (p's<0.0002), but computed and published raw modes were indiscriminable ($p<0.15$).

Predicting Export of Arctic Sea Ice

The export of Arctic sea ice through the Fram Strait off northeast Greenland is an important factor in the freshwater balance of the North Atlantic Ocean, and affects the North Atlantic thermohaline circulation. The January monthly ice export at fluxgate *a* of the Fram Strait[8] was studied using the ipsative modes found here. The data consisted of sea ice area flux for the years 1979-2002. Kendall's tau b statistic was used to determine the correlation of modes with ice export, and the significant associations are shown in Figure 5. Negative associations were found with ipsative modes U (over Greenland), CC (near Svalbard), 3 (near Franz Josef Land), XX (off the coast of northern Norway), and SS (eastern Pacific Ocean). Positive associations were found with ipsative modes UU (Mediterranean Sea south of France), WW (North Atlantic Ocean northwest of Spain), H (over Manchuria), and BB (east of Japan).

An example of a pattern with high sea ice export is illustrated in Figure 6. The 500 mb pattern in January 1983 yielded the maximal ice export for any January in the years of 1979-2002. Low 500 mb heights extend from Greenland to Scandinavia and western Russia, and another area of low heights is found off of the Pacific coast of the USA. Areas of high 500 mb heights are seen over southwest Europe and the western Mediterranean Sea, and over Mongolia and northeast China.

2155-0182/10/$3.00

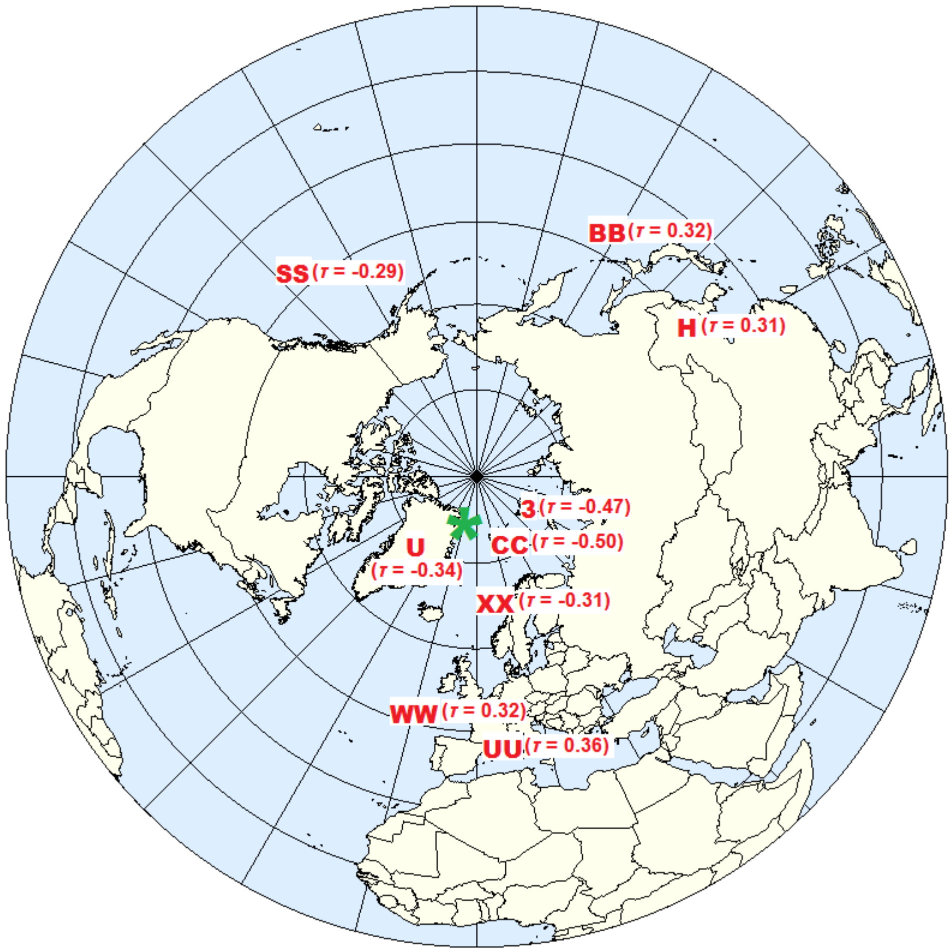

Figure 5: Ipsative modes and Kendall's Tau b Coefficients with Statistically Significant (p<.05) Associations with Ice Export at Fram Strait Fluxgate *a*, Indicated as *

Recent research[9] reported no correlation between SLP-based NAO and Arctic wintertime sea ice export over 1958-1977, and a positive correlation of 0.7 over 1978-1997. An eastern shift in NAO centers of variability was suggested to explain this phenomenon. However, for the 500 mb level, ipsative mode U was a stable center over Greenland, for both sets of years, 1948-1976 and 1977-2007. Mode U represents the northern center of the NAO dipole at the 500 mb level. Mode II (near Iceland) was also a stable center, coincident with the northern center of surface-level winter NAO variability: this does not support the idea of a shift at 500 mb. Furthermore, factors XX, CC and 3, located in this region, were stable in both eras and reliably associated with sea ice movement. Mode 3 is coincident with the surface center of variability in the Kara Sea, previously found to be associated with sea ice export variability.[10]

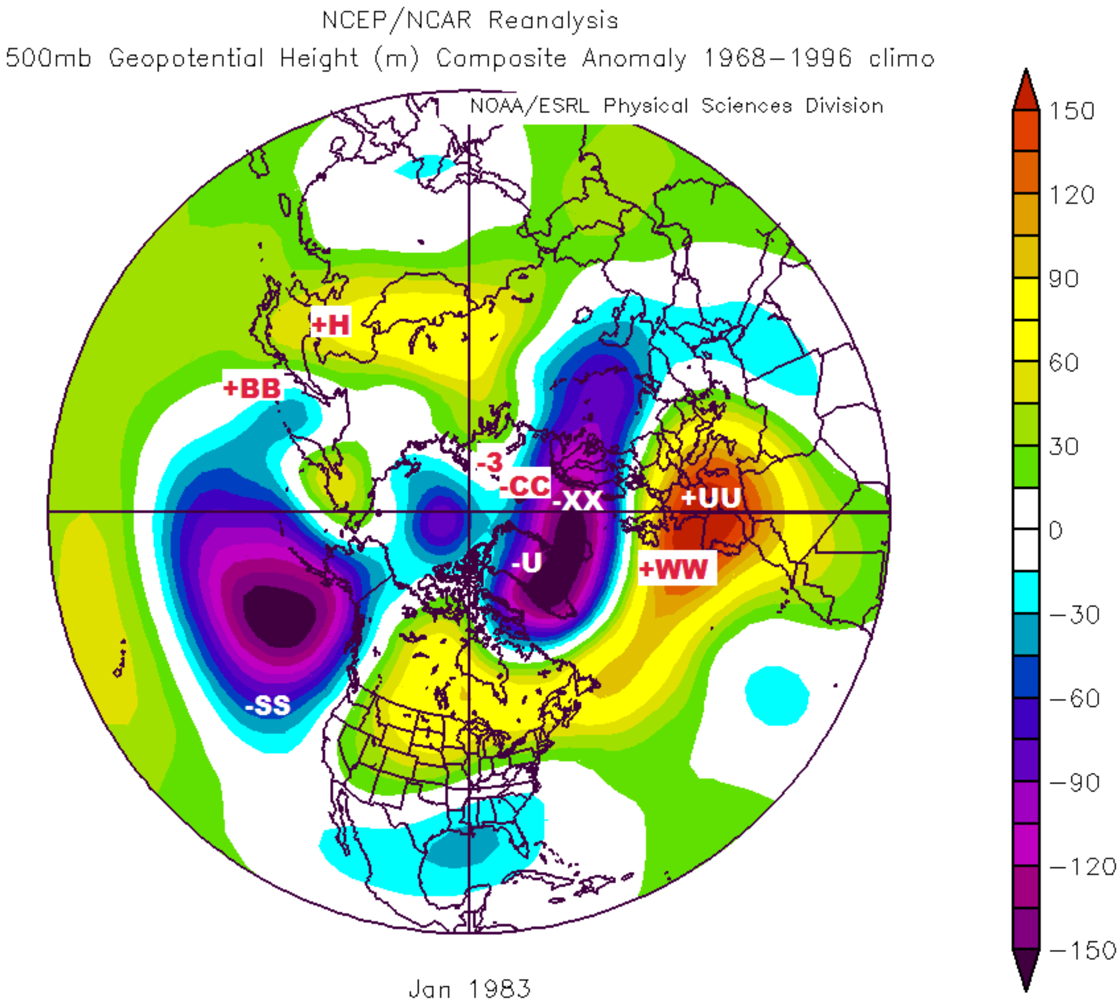

Figure 6: 500 mb GHA for January 1983, which Entailed the Maximal January Ice Export for the Period 1979-2002: Ipsative modes are Prefixed by the Sign of their Associated Kendall's Tau b Coefficient

Epilogue

Preliminary results using uncounfounded climatic data in atmospheric prediction are very positive. An important extension of the present research is obtaining GHA modes for all months of the year. Further evaluation of optimal statistical methods used with unconfounded climatic data is warranted. Future research should use these data in applications such as, for example: predicting the ontogenesis, intensity, and path of hurricanes[11], and the ontogenesis, intensity, and location of sudden stratospheric warmings[12,13]; modeling of seasonal energy consumption and management of climate risk for energy firms[14]; forecasting and understanding the ENSO cycle (El Niño)[15], and development and evaluation of numerical weather prediction models.[16]

2155-0182/10/$3.00

References

[1]Yarnold PR. Characterizing and circumventing Simpson's paradox for ordered bivariate data. *Educational and Psychological Measurement* 1996, 56:430-442.

[2]Barnston AG, Livezey RE. Classification, seasonality and persistence of low-frequency atmospheric circulation patterns. *Monthly Weather Review* 1987, 115:1083-1126.

[3]Bryant FB, Yarnold PR. Principal components, and exploratory and confirmatory factor analysis. In: LG Grimm, PR Yarnold (Eds.), *Reading and understanding multivariate statistics*. APA Books, Washington, DC, 1995, pp. 99-136.

[4]Yarnold PR. Statistical analysis for single-case designs. In: FB Bryant, L Heath, E Posavac, J Edwards, E Henderson, Y Suarez-Balcazar, and S Tindale (Eds.), *Social psychological applications to social issues, volume 2: methodological issues in applied social research*. Plenum, New York, NY, 1992, pp. 177-197.

[5]Yarnold PR. Discriminating geriatric and non-geriatric patients using functional status information: an example of classification tree analysis via UniODA. *Educational and Psychological Measurement* 1996, 56:656-667.

[6]Yarnold PR, Soltysik RC. *Optimal data analysis: a guidebook with software for Windows*. Washington, DC, APA Books, 2005.

[7]Cade BS, Richards JD. *User manual for blossom statistical software*. US Geological Survey, Fort Collins, CO, 2005.

[8]Kwok R, Cunningham GF, Pang SS. Fram Strait sea ice outflow. *Journal of Geophysical Research* 2004, 109:1009-1029.

[9]Holland MM. The north Atlantic oscillation–Arctic oscillation in the CCSM2 and its influence on Arctic climate variability. *Journal of Climate* 2003, 16:2767–2781.

[10]Hilmer M, Jung T. Evidence for a recent change in the link between north Atlantic oscillation and Arctic sea ice export. *Geophysical Research Letters* 2000, 27:989–992.

[11]Willoughby HE, Rappaport EN, Marks FD. *Hurricane forecasting: the state of the art*. *Natural Hazards Review* 2007, 8:45-49.

[12]Charlton AJ, Polvani LM. A new look at stratospheric sudden warming events: part I. climatology and modeling benchmarks. *Journal of Climate* 2007, 20:449-469.

[13]Charlton AJ, Polvani LM, Perlwitz J, Sassi F, Manzini E. A new look at stratospheric sudden warming events: part II. evaluation of numerical model simulations. *Journal of Climate* 2007, 20:470-488.

[14]Troccoli A (Ed.). Management of weather and climate risk in the energy industry. Proceedings of the NATO advanced research workshop on weather/climate risk management for the energy sector, Santa Maria di Leuca, Italy 6-10 October 2008. Series: *NATO science for peace and security series C: environmental security*. Springer, New York, NY, 2008.

[15]Babkina AM (Ed.). *El Niño: overview and bibliography*. Nova Science Publishers, Hauppauge, NY, 2004.

[16]Kalnay E. *Atmospheric modeling, data assimilation and predictability*. Cambridge University Press, Cambridge, UK, 2002.

Author Notes

Send correspondence to the authors at: Optimal Data Analysis, 1220 Rosecrans St., Suite 330, San Diego, CA 92106. Send E-mail to: Journal@OptimalDataAnalysis.com.